Solid-State ^{13}C NMR of Liquid Crystalline Polyesters: Variations in Morphology, Alignment, and Dynamics within a Homologous Series

Dan McElheny, Julia Grinshtein, Veronica Frydman, and Lucio Frydman*

Department of Chemical Physics, Weizmann Institute of Sciences, 76100 Rehovot, Israel, and Department of Chemistry, University of Illinois at Chicago, Chicago, Illinois 60607-7061

Received October 25, 2001; Revised Manuscript Received January 16, 2002

ABSTRACT: The local ordering, morphology, and dynamics of aromatic cores and flexible alkyl spacers were analyzed for a homologous series of main-chain polymeric liquid crystals. ^{13}C NMR experiments showed that the nematic ordering achieved by these synthetic polymers was retained into the solid state if their quenchings occur while remaining within the strong NMR magnetic field. The degree of orientation in the resulting glasses was investigated by variable-angle NMR experiments and found to differ between polymers with an even number of methylene units in the flexible spacer vs those with an odd number. To further discern at a molecular level the nature of these differences, the structures of these polyesters were examined by high-resolution solid-state ^{13}C NMR. It was found that while the odd-chained series displayed a conformational annealing upon aligning, even-chained polymers were generally in all-trans conformations both for as-synthesized and for aligned samples. Variable-temperature 1D and 2D NMR experiments also illustrated substantial differences in the degree of motional dynamics between the odd and even polymer series: whereas considerable rigidity was exhibited by the even-numbered series all the way up to 150 °C, a relatively high flexibility displayed by the odd-methylene polymers. In unison, these measurements provide insight into the significant changes that can be imparted into the structure and dynamics of main-chain thermotropic polymers by subtle manipulations of their monomeric structures.

1. Introduction

Stimulated by the interesting properties and practical applications of liquid crystalline polymers (LCPs), recent years have seen considerable efforts directed at furthering the development and understanding of these materials.[1−7] Whereas most electronic and optical developments involving LCPs rely on structures where mesogenic groups are pending from the polymer backbone,[1−10] material applications have generally focused on main-chain LCP arrangements. Mesogenic cores are here placed along the main polymer backbone and endowed with a flexibility which largely defines the processing characteristics of the macromolecule. For instance, rigid polyamides such as Kevlar, possessing strongly conjugated aromatic groups along their main chains, require strong caustic solvents for generating a nematic phase.[4,5] By contrast, other commercial LCPs such as Vectra and X7G, having ester linkers replacing the aramides' amide moieties and incorporating alkyl spacers in between the aromatic cores, only require heat to reach the liquid crystalline state.[10,11] By carefully choosing the type of mesogen and spacer incorporated into the backbone of these thermotropics, the degree of liquid crystalline order as well as the arrangement adopted by these macromolecules (nematic, smectic, cholesteric) can be controlled. A number of variations on such LCP structures have resulted in the proposal of advanced thermotropic materials with commercial applications.[7] Processing these main-chain LCP is also often reliant on the application of external fields, which align the macromolecular domains within the liquid crystalline solution into uniformly ordered systems. Defining characteristics of LCP material applications are consequently a polymer's ability to generate mesomorphic phases, to become macroscopically aligned by the application of external fields, and to retain its ordered structure at both a microscopic and a macroscopic level when subsequently frozen into the glassy state. Also of basic interest is to quantify the degree of mobility characterizing the polymer chains in the solid, as this will affect the aging properties and the durability of the ordered materials.

The present work focuses on monitoring the interplay between monomeric structures and these various defining properties of LCPs at a site-resolved level. Our particular objective was to employ an atomic-level probe such as NMR in order to monitor how subtle changes in monomeric structure could affect the conformation, orientational arrangements, and dynamics of thermotropic LCPs. Rather than focusing on complex chemical mixtures such as those involved in commercial copolymeric LCPs, our analyses centered on the well-defined synthetic series depicted in Scheme 1. These thermotropic polyesters were developed in the early 1980s by Lenz and co-workers[12,13] and exhibit the advantage of sharing several material properties in common with commercial LCPs while allowing for systematic structural changes. A number of physical and spectroscopic characterizations have actually been reported for these systems. These include variable-temperature birefringence measurements, vibrational spectroscopy, and transmission electron microscopy studies,[14−17] as well as solid-state NMR investigations on the $n = 6$ derivative.[18,19] The former showed that the spacers may play a nontrivial role in determining the organization of the solid state, whereas the latter revealed a dependence of the macromolecule's conformation on the crystallization/quenching conditions used to obtain a solid sample.

We extend here the insight arising from these previous studies by means of isotropic and anisotropic NMR observations of chemically inequivalent sites within a

* To whom correspondence should be addressed: phone +972-8-9344903; FAX +972−8−9344123; e-mail lucio.frydman@weizmann.ac.il.

10.1021/ma011863v CCC: $22.00
Published on Web 03/27/2002

Scheme 1

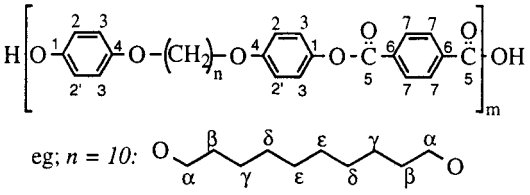

eg; *n* = 10:

homologous polymer series with $n = 5-10$. By measuring chemical shielding anisotropy (CSA) ^{13}C line shapes, the degree of alignment for aliphatic and aromatic groups could be estimated before and after quenching the LCPs into an ordered glassy state. High-resolution solid-state ^{13}C NMR could then be employed in order to extract, via observations of the characteristic isotropic chemical shifts of individually resolved resonances, various conformational arrangements that polymers adopt upon being quenched into solids. Finally, variable-temperature 1D and 2D high-resolution ^{13}C techniques were employed to carry out a site-resolved characterization of the motional dynamics occurring for selected members within the polymer series in the solid state. The following sections describe the results obtained during the course of such experiments as well as the interplay that they revealed between the chemical structure of thermotropic macromolecules and their morphology, order, and dynamics.

2. Experimental Section

The synthetic approach followed for preparing the samples analyzed throughout this work was taken from the description given by Lenz and Griffin et al (Scheme 2).[12,13,20] The resulting polymers were obtained as white solid powders, and their mesophasic behavior was monitored prior to the actual NMR studies by differential scanning calorimetry (Mettler DSC-30 calorimeter) and via optical means. The transition phase characteristics displayed by these synthetic samples were in good agreement with those reported in the original synthetic studies.

First among the NMR experiments that were carried out was a series of melt/quench procedures, which monitored the bulk degree of alignment achieved by the different chemical groups within the LCP structures upon freezing the ordered mesophases into glasses in a sudden fashion. To carry out such experiments, 50 mg of as-synthesized polymers was loaded into custom-made 5 mm o.d. Pyrex tubes and placed into a specialized variable director probehead where their subsequent NMR investigation took place (Figure 1). Once the probe was inserted inside the magnet these powders were heated within a ceramic chamber with a steady stream of nitrogen gas to the desired mesogenic temperatures, usually within the 245−290 °C range. This heating process was monitored using a thermal controller as well as via the acquisition of static ^1H and ^{13}C NMR spectra at resonance frequencies of 201 and 50.5 MHz, respectively. Upon melting into liquid crystalline phases, the samples exhibited distinct sets of sharp resonances away from their isotropic chemical shifts; once these were observed, the nematic fluids were allowed to equilibrate under the influence of the NMR magnetic field for at least 1 h to ensure a complete alignment of these mesophases. A sudden external stream of nitrogen gas cooled to −196 °C was then introduced into the gas flow, which resulted in a rapid (∼5 °C/s) drop in the temperature and a quenching of the oriented samples into their glassy state.

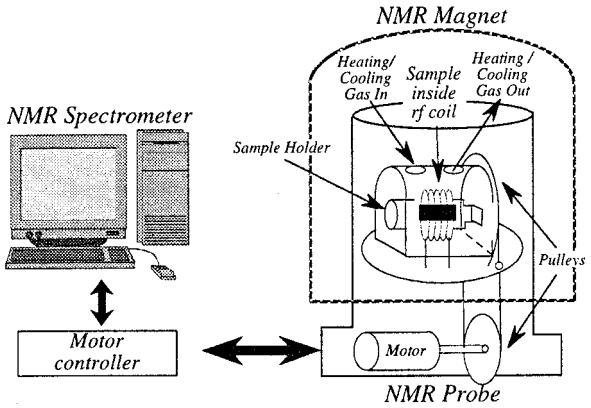

Figure 1. Experimental setup employed in the 1D variable-director ^{13}C NMR acquisitions. The NMR probe head design allows for $N_2(g)$ to flow from either hot or cold reservoirs into an insulated chamber containing the sample tube, and to eventually exit through the top of the magnet. To carry out the variable-director NMR experiments, sample glass tubes were provided with custom square-shaped ends which tightly fit into a ceramic pulley system, connected in turn via high-tensile Kevlar strings to a stepping motor positioned at the base of the probe. This motor (and its optical encoder assembly) controlled the sample's reorientation as commanded by an intelligent PC-based controller system, proceeding itself under the timing guidance of the spectrometers pulse programmer.

A number of alternative NMR techniques were assayed on such quenched samples in order to quantify their degree of molecular alignment. One such method involved the collection of 2D spectral correlations between two orthogonal sample orientations;[21−23] another strategy involved monitoring anisotropic powder line shapes for each chemically inequivalent site via 2D isotropic−anisotropic correlation techniques.[24,25] Yet when applied to the present set of LCPs each of these methods exhibited its own drawback; the first one in terms of signal-to-noise sacrifices and the latter due to its requirement for replacing the sample into a spinner and thus risking disturbances in the alignment. In fact, it was concluded that the most practical and reliable approach for implementing our ordering characterizations resulted from repeating basic static ^{13}C NMR experiments, not just at the single orientation resulting upon first quenching the polymer but as a function of the angle ψ between the main axis of alignment and the

Scheme 2

Monomer Synthesis:

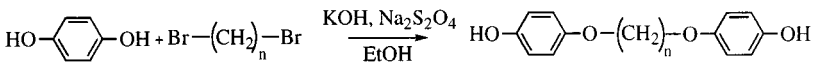

1

Polymer Synthesis:

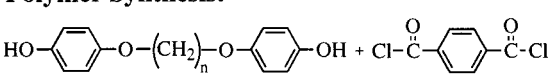

1

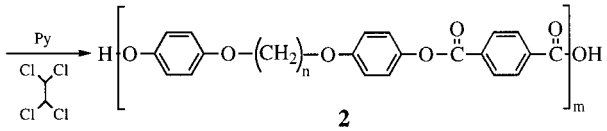

2

NMR magnetic field B_0. Although such variable-angle ^{13}C static measurements lacked high spectral resolution they possessed a high angular reproducibility—the aligned samples were never actually withdrawn from the magnet—as well as good signal-to-noise (no need for intermediate storage periods). To assess orientational alignment from these variable-director experiments, an a priori knowledge of the CSA tensor parameters characterizing each ^{13}C chemical site in the monomer is needed. Such information was retrieved for this study from 2D variable-angle correlation spectroscopy (VACSY) experiments, capable of resolving static-like CSA line shapes according to each site's isotropic chemical shift. This technique involves acquiring the signals arising from a fast spinning sample as a function of different angles ψ between the axis of macroscopic rotation and the external field B_0. These time-domain NMR signals can then be regarded as implicit functions of a time-domain vector $[t, P_2(\cos\psi)t]$, t being the actual acquisition time of the signal. A bidimensional Fourier transformation of these signals against such vectors

$$I(\omega_{iso},\omega_{aniso}) = \int\int S(\psi,t)\exp\{-i[\omega_{iso}t + \omega_{aniso}P_2(\cos\psi)t]\}\,dt\,d[P_2(\cos\psi)t] \quad (1)$$

then affords the desired $I(\omega_{iso},\omega_{aniso})$ 2D correlation spectrum separating the anisotropic powder patterns $I(\omega_{aniso})$ against each site's isotropic chemical shift ω_{iso}. Additional pulse sequence details employed in these experiments are given below; data processing protocols for setting up and implementing such experiments have also been described elsewhere in detail.[26]

In addition to the variable-angle experiments, a variety of ^{13}C magic-angle-spinning (MAS) NMR experiments were also carried out on both as-synthesized and magnetically aligned samples. One goal of such measurements was to assess what conformational changes, if any, had been experienced by the polymer chains upon being melted and then aligned in the magnetic field. Another of our goals was to assess the nature of local motions throughout the polymer series, as viewed by each inequivalent monomer site as a function of the spacer's length. To retrieve this information, a series of variable-temperature 1D CPMAS and 2D separated-local-field (SLF) ^{13}C NMR spectra were collected. The first set of experiments yielded insight into the ongoing motions via the coalescence of chemical inequivalencies arising from the polymers' various conformers, and were conducted using conventional cross-polarization sequences. All isotropic chemical shifts in these high-resolution solid NMR experiments were referenced to $\delta_{TMS} = 0$ ppm using adamantane as external reference. The second group of experiments provided motional information about individual protonated ^{13}C sites from the intensities of their $^{13}C-^{1}H$ sideband manifolds, which appear along an indirectly encoded spectral dimension and therefore do not compromise the isotropic shift resolution afforded by MAS. As further described in the original literature, these dipolar manifolds reflect the effective $^{13}C-^{1}H$ couplings felt by each carbon site;[27−30] since the distances defining these dipolar couplings are nearly constant for all bonded $^{1}H-^{13}C$ pairs, changes observed in these sideband line shapes with temperature provide unambiguous information about the onset of motions at each molecular position. A number of pulse sequences have been proposed and demonstrated for acquiring such data;[27−30] for the sake of simplicity, we employed for our measurements a recently proposed variant applicable in the moderately fast MAS regime, which does not require the implementation of homonuclear decoupling among protons.[31]

3. Results and Discussion

3.1. Variable-Angle ^{13}C NMR of Partially Aligned Polyester Samples. As mentioned, one of the aims of this study involved monitoring the degree of alignment achieved by the polymers in Scheme 1 upon being melted into their mesophase as well as the order retained upon suddenly quenching them into a glassy state. An idea about the significant changes that these LCP transitions will impart on static ^{13}C NMR spectra is offered in Figure 2, which shows how the traces from an $n = 6$ sample changed between an as-synthesized random sample, after melting this into an LC state, on quenching this back to room temperature inside the NMR magnetic field, and on reorienting the director of such aligned glass perpendicular to the B_0 magnetic field. In all instances the site-specific NMR resonances are defined by the sum of isotropic and anisotropic chemical shift contributions, yet it is clear that the orientational and dynamic characteristics of the sample will also be defining factors in the spectral line shapes observed. In particular, analyzing the ^{13}C resonance shifts and powder pattern distortions observed in Figure 2C,D can provide a detailed information regarding the degree of order adopted by a polymer upon aligning. Needed for implementing such ordering analyses are the unaveraged components of the CSA associated with each site in the monomer, in terms of both their magnitude

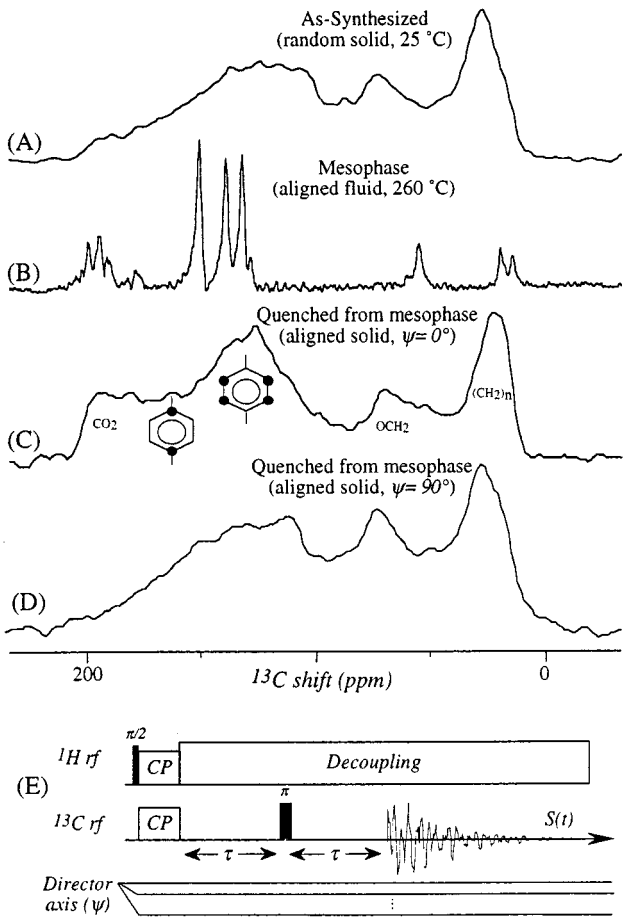

Figure 2. Static 1D ^{13}C NMR spectra recorded for the $n = 6$ LCP in its semicrystalline form (A), upon being melted into the nematic state (B), after being suddenly quenched back down to room temperature while remaining in the NMR magnet (C), and on reorienting this aligned sample by 90° with respect to B_0 (D). The pulse sequence employed for the acquisition of the variable-angle static ^{13}C NMR experiments involved cross-polarization (CP) at 50 kHz Hartmann−Hahn matching conditions, contact times of 1 ms, continuous wave ^{1}H decoupling at rf fields of 80 kHz, and a spin echo to avoid dead time problems leading to artificial spectral distortions (E). A laboratory-built 4.7 T NMR spectrometer was utilized for these measurements; the trace in (C) illustrates the qualitative chemical origin of various spectral bands.

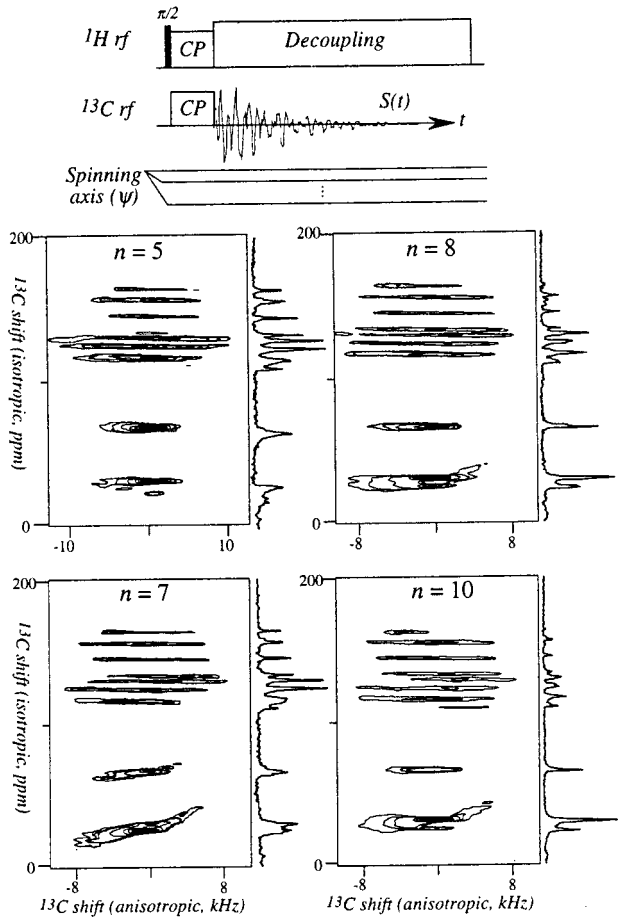

Figure 3. 2D ^{13}C VACSY NMR spectra recorded on selected polymers with $n = 5-10$ at room temperature, shown as equidistant contour plots between 5 and 40% of the maximum signal intensity. Illustrated along one of the axes are the isotropic projections of the spectra; correlated along the orthogonal dimension are the shielding anisotropy patterns from which the tensor values reported in Table 1 could be extracted by numerical fitting. A laboratory-built 7.1 T NMR spectrometer was utilized for these measurements, along with a custom variable-angle-spinning probe. Sample spinning orientations were controlled to within 0.1° using an assembly similar to the one depicted in Figure 1, albeit incorporating a 5 mm Doty Scientific pneumatic module capable of sample rotation rates in excess of 8 kHz. These acquisitions involved the pulse sequence schematized on top, with CP from protons for 2.5 ms contact times, nutation fields of 70 kHz, and 31 spinning angles ψ distributed over the 35°−90° range in constant $\Delta[P_2(\cos\psi)] = 0.033$ increments.

and their orientations. These values were extracted in this work from ambient 2D VACSY spectra that display along one of their dimensions the high-resolution ^{13}C trace of each sample and along the other dimension the staticlike CSA line shape of each inequivalent site (Figure 3). Given the similarities that we observed among the CSA parameters resulting from homologous sites in these various 2D spectra coupled to the fact that spectral resolution between sites deteriorated with the spacer's length (particularly for $n \geq 7$), these VACSY data were used to derive "prototypical" shielding values for various types of aliphatic, aromatic, and carbonyl ^{13}C sites. These values are summarized in Table 1; the orientations (α, β, γ) assumed for the principal axes systems (PASs) of each chemically inequivalent site were set in accordance with literature guidelines.[32,33]

With an a priori knowledge of the individual CSA parameters, the NMR line shape arising from each ^{13}C site in the oriented polymer samples can be calculated as a function of the angle ψ between the main axis of alignment and the NMR magnetic field B_0 as

$$\omega(\psi) = \omega_{iso} + \omega_{aniso}(\Omega)P_2(\cos\psi) \qquad (2)$$

where $P_2(\cos\psi) = (3\cos^2\psi - 1)/2$ is the second-order Legèndre polynomial, ω_{iso} represents the isotropic chemical shift for the particular site, and the anisotropic contribution ω_{aniso} depends on the site's CSA parameters as well as on its relative orientation Ω with respect to the alignment axis. To deal with the complex multisite monomeric structures considered in this work, we found it convenient to describe these orientations with the aid of an intermediate molecular frame of reference (MF), fixed along the idealized main axis of a monomer unit.[23,34] The complete transformation leading from each site's PAS to the main magnetic field B_0 was thus assembled as

$$\text{PAS} \xrightarrow{(\alpha,\beta,\gamma)} \text{MF} \xrightarrow{(0,\theta,\phi)} \text{DF} \xrightarrow{(0,\psi,0)} \text{LF} \qquad (3)$$

where the (α, β, γ) set is fixed for each site, the orientations (0, θ, ϕ) describe the orientational distribution characterizing each monomer frame with respect to the overall sample director, and the orientation ψ between the director's frame (DF) and the laboratory frame (LF) is the parameter that we experimentally controlled via the mechanical stepping motor. Our main interest thus centered on determining the distribution assumed by the (θ, ϕ) angles, which could in principle range from a single value for a single crystal up to a uniform solid sphere distribution for a random powder. In the present work, this distribution was modeled on the basis of the uniaxial function[33,34]

$$P(\theta) = \exp(-\sin^2\theta/2\sigma_\theta^2) \qquad (4)$$

Using a single σ_θ value for describing the Gaussian-like ordering distributions for all sites in a monomer would actually be too naive an assumption, as it would not allow for any of the internal flexibility that is known to characterize spacer-based main chain LCPs. To account for this feature the specific σ_θ values assumed for the aliphatic, mesogenic (diphenoxy, terephthalic, and carbonyl) and methoxy moieties were allowed to differ within each monomer. In such manner, site-specific degrees of orientational alignment could be evaluated while preserving the overall simplicity of the model.

Table 1. Prototypical ^{13}C Chemical Shift Tensor Parameters Measured for the LCP Series[a]

site[b]	δ_{iso} (ppm)	δ_{11} (ppm)[c]	δ_{22} (ppm)[c]	δ_{33} (ppm)[c]
1	155	245	164	66
2,2′	116	176	146	26
3	123	203	145	21
4	144	238	97	97
5	163	267	111	111
6	133	231	138	30
7	129	262	156	-31
α	67	87	87	27
$\beta(\delta,\epsilon)$[d]	31	47	31	15
γ	24	37	24	11

[a] Isotropic solid-phase shifts considered accurate within ±0.5 ppm; individual tensor values accurate within ±3 ppm. [b] Following the numbering described in Scheme 1. [c] Under the convention, δ_{11} = most deshielded element and δ_{33} = most shielded element. [d] For $n \geq 7$ similar parameters were assumed for all these sites.

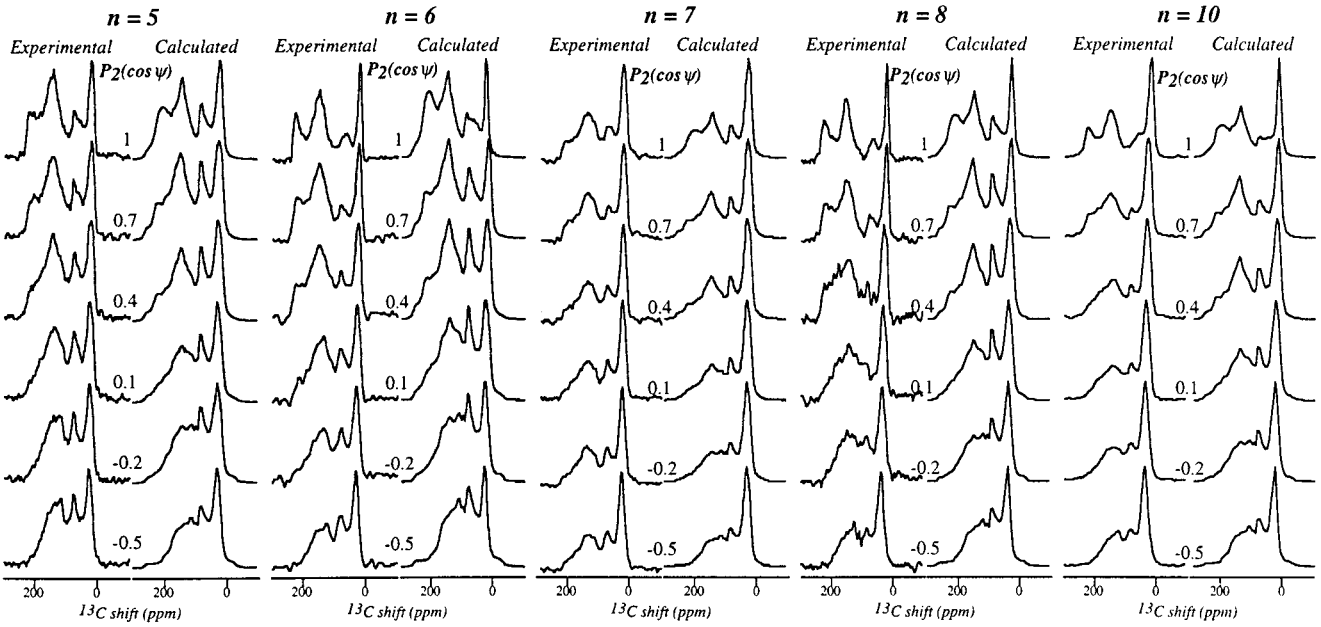

Figure 4. Comparisons between experimental variable-director ^{13}C NMR spectra recorded for aligned $n = 5-10$ polymer samples after being quenched from their melts and best-fit simulations based on the formalism described in the text. Spectra were recorded at room temperature as a function of sample orientation ψ using the indicated $P_2(\cos \psi)$ values; the parameters employed for obtaining the simulated distributions are reported in Table 2.

Equipped with these experimental and theoretical protocols, the variable-angle ^{13}C NMR spectra acquired for the $n = 5-10$ polymer series were examined. Figure 4 illustrates the NMR results obtained from these aligned glasses as a function of their macroscopic orientations ψ with respect to B_0; best fit spectral simulations are also shown to the side of each experiment. It is important to notice that on computing these simulations all the sites' relative abundances as well as their different isotropic and anisotropic shielding parameters were predetermined, and only the σ_θ values assumed for the mesogenic, methoxy, and aliphatic portions of the monomers had to be varied through the fit. In view of this restriction and of the relative simplicity of our model, it is satisfying to note the good agreement that simulated line shapes show with the experimental spectra. The main differences between the two sets seem to arise within the spectra of the most highly oriented samples, in particular within the mesogenic regions of polymers $n = 6$ and $n = 8$. At this point it is not entirely clear whether these differences reflect the very simple distribution function $P(\theta)$ adopted for the simulations—other distribution functions were assayed but did not yield considerable improvements in the fit—or are the consequence of unaccounted variabilities within the polymers' mesogenic groups (differences in internal alignment, multiple internal conformations, etc.). Despite these minor discrepancies, it is clear that these experiments provide sufficient quantitative insight into how ordering changes for the various segments of the homologous polymer series; the best-fit values obtained for the various ordering parameters of chemically inequivalent groups are reported in Table 2.

One of the features stemming from these characterizations is the relatively high degree of alignment that all LCPs retain upon being frozen from their nematic melts. For instance, anisotropic displacements of the ^{13}C NMR resonances in the nematic phase (e.g., Figure 2B) reveal for the $n = 5$ polymer an overall order parameters

Table 2. Orientational Distribution Values Observed for Various Chemical Moieties in $n = 5-10$ LCP Samples after Quenching from Nematic State

	σ_θ distributions (deg)[a]		
n	alkyl spacer	$-OCH_2-$	mesogen
5	20 ± 20	30 ± 15	15 ± 5
6	10 ± 20	25 ± 20	5 ± 5
7	25 ± 20	30 ± 15	15 ± 5
8	15 ± 20	30 ± 20	6 ± 5
10	15 ± 20	30 ± 15	10 ± 10

[a] Error values denote ranges of angular distributions compatible with equal-quality fits of the experimental spectra.

$\langle S_{zz} \rangle \approx 0.8$, a value which increases even a bit further for $n = 6$. Average mesogenic σ_θ values can be used to estimate corresponding order parameter values for the polymers in the oriented glassy state; these follow from eq 4 as

$$\langle S_{zz} \rangle = \int P_2(\cos \theta) P(\theta)\, d\theta \qquad (5)$$

The experimental solid spectra then also lead to average order parameter $\langle S_{zz} \rangle \approx 0.8-0.9$ for the mesogenic groups of these polymers. Another distinctive feature arising from the solid spectra concerns the even–odd alternation displayed by the polymer series' order parameters. Actually, even a superficial comparison among the experimental variable-angle spectra shows—particularly for the ^{13}C line shapes arising from the mesogenic groups—sharper spectral features for even-numbered members of the series than for the odd-numbered ones. These differences result from enhancements in the alignment which can in turn be attributed to packing effects, according to which polymers with an even number of methylenes in their spacers can align properly along the direction of the main macromolecular axis whereas those with $n =$ odd cannot unless certain methylene groups depart from their preferred all-trans conformations (Scheme 3).[35-37] Such conformational variations would occur at the expense of sacrifices in

Table 3. ^{13}C Isotropic Shifts Observed for Various Chemical Sites throughout the $n = 5-10$ LCP Series

	aromatics								aliphatics				
n,sample	1	2	2′	3	4	6	7	CO/5	α	*β*	*γ*	*δ*	*ϵ*
5,as synthesized[a]	156.0	111.0	116.5	124.0	145.0	133.5	130.0	164.0	67.5	31.5	24.0		
										28.0	21.5		
5,aligned[a]	156.0	111.0	117.0	124.5	145.0	133.0	129.5	163.5	67.5	32.0	24.0		
									71.5		21.5		
5,isotropic[b]	157.9	116.6	116.6	122.8	145.4	132.0	131.2	167.6	67.3	28.3	21.9		
6, as synthesized[a,c]	155.5	111.5	117.0	124.0	144.5	133.5	130.0	163.5	67.5	32.0	27.0		
6, aligned[a,c]	155.5	111.5	117.0	124.5	145.0	133.5	130.0	164.0	68.0	32.5	27.5		
7, as synthesized[a]	155.5	111.5	117.0	124.0	145.0	133.5	130.0	163.5	67.5	32.5	28.5	30.0	
			115.5						66.5		26.5		
									71.5				
7, aligned[a]	156.0	111.5	117.5	124.5	145.0	133.5	130.0	164.0	67.0	33.0	28.0	30.0	
			115.5						71.5		26.5		
									74.0				
8, as synthesized[a]	155.5	111.5	117.0	124.5	145.0	133.5	130.0	163.5	67.5	33.0[d]	27.5	33.0[d]	
		110.5	115.5								26.3		
8, aligned[a]	155.5	111.5	116.5	124.0	144.5	133.0	129.5	163.0	68.0	32.5[d]	27.5	33.0[d]	
									67.5	30.0[d]		30.0[d]	
10, as synthesized[a]	156.0	112.0	117.0	123.5	145.0	134.0	130.0	162.5	67.5	33.0[d]	26.5	33.0[d]	33.0[d]
		110.5		125.0									
10, aligned[a]	155.0	110.5	116.0	123.5	144.0	132.5	129.0	163.0	67.5	32.5[d]	27.0	32.5[d]	32.5[d]
									67.0				

[a] From Figure 5. [b] Isotropic shifts (±0.1 ppm) recorded for the monomer precursor in $CDCl_3$. [c] Shifts identical, within experimental error, to those reported in ref 18. [d] Assignments ambiguous within the spacer's chain.

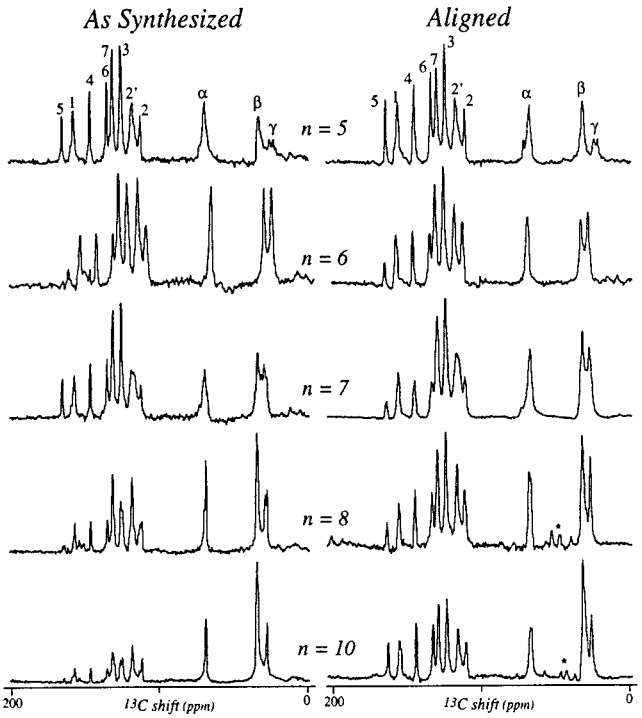

Figure 5. Comparison between the high-resolution solid-state ^{13}C NMR spectra arising from the as-synthesized and aligned polymer samples. The peaks' assignment corresponds to the sites indicated in Scheme 1, and their shifts are listed in Table 3. All spectra were collected on a laboratory-built spectrometer and probe at 50.5 MHz using a CP sequence (1 ms contact time, Hartmann−Hahn matching at 66 kHz), 80 kHz TPPM decoupling, and 5−6 kHz MAS rates. Typically 2048 scans were acquired with a 3 s recycle delay; asterisks denote spinning sidebands.

the optimum packing conditions, leading to the alternating macroscopic alignment values σ_θ observed by NMR. Finally, it is interesting to consider the systematic differences that variable-director experiments reveal for the ordering of the various groups within the monomeric LCP units. As expected, narrower σ_θ distributions are detected for the mesogenic aromatic cores than for the flexible spacers. Unusual, however, is the higher degree of disorder observed in all samples for the methoxy resonance, which one would expect intermediate between the alkyl and aromatic values. Yet CPMAS spectra also evidence the presence of inequivalencies within the $-OCH_2-$ groups upon aligning the polymer samples (Figure 5); when taken in unison, these data suggest that a higher degree of conformational variability may be characterizing the methoxy groups than the remainder methylenes in the alkyl chains.

Scheme 3

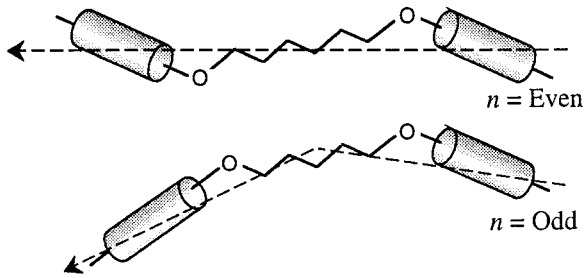

3.2. High-Resolution Solid-State NMR of Thermotropic Polyesters: Conformational Differences between Random and Aligned Samples. As part of the overall polymer aligning process, conformations might change between the random environments in which samples are initially synthesized and their subsequent quenching as ordered solids from the liquid crystalline phase. Such conformational changes could in turn be reflected in the polymers' solid NMR spectra. Working on this premise, polymer samples that were aligned and quenched inside the NMR magnetic field were subsequently compared via high-resolution CP-MAS NMR against the starting random materials. The resulting spectra are shown in Figure 5, and the isotropic chemical shift values observed for various inequivalent sites are reported in Table 3. Also shown in the table as aids in resonance assignment are the corresponding shift values observed for inequivalent sites in the $n = 5$ soluble monomer precursor.

When comparing within these sets the as-synthesized spectral series with the quenched one, odd-chained polymers show slightly sharper alkyl features indicative of an increased homogenization in their spacers' packing. Significant narrowing is also evident upon annealing for the mesogen core resonances of the $n = 6-10$ samples. The only exception to this narrowing trend

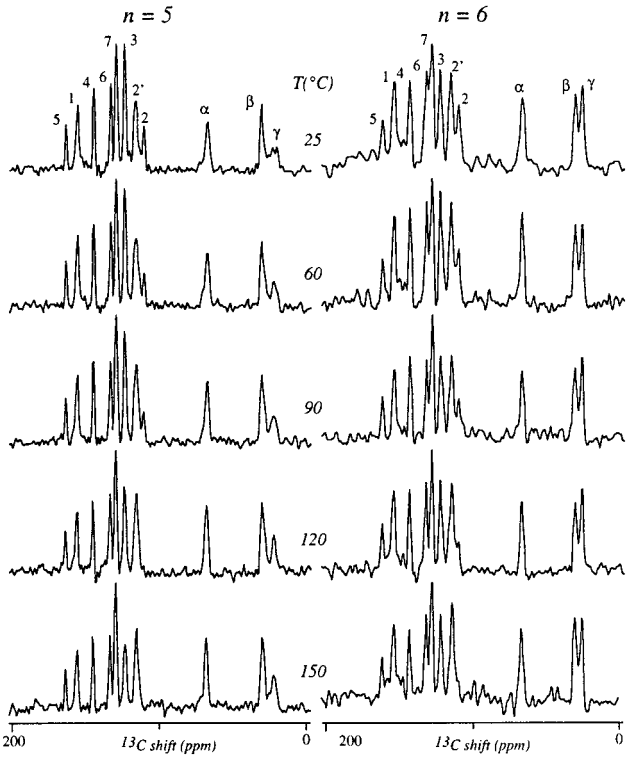

Figure 6. Variable-temperature ^{13}C CPMAS spectra observed for $n = 5$, 6 as-synthesized polymer samples. Data were collected on a 7.1 T laboratory-built spectrometer at 78.5 MHz using similar conditions as in Figure 5, yet with MAS rates of 12 kHz.

appears in the methoxy resonances, which broaden and even split for certain samples upon the annealing. A systematic difference is also noticed between the alkyl regions of odd- and even-numbered LCPs; the former show more complex patterns for their methylene resonances in both random and aligned samples, as could be expected from the more heterogeneous conformational distribution of spacer chains suggested in Scheme 3.

3.3. 1D and 2D CPMAS Analyses of Segmental Dynamics. The differences noticed between both static and CPMAS NMR spectra of even- and odd-numbered LCPs suggest differences in the conformations adopted by their macromolecular chains. Since the degree of conformational order will also define the interchain packing efficiency and thus the free volume available for macromolecular relaxation, such differences can also be expected to affect the polymers' local dynamics. To investigate this dynamic feature of the LCP series, a series of 1D and 2D NMR experiments were carried out on the $n = 5$ and $n = 6$ polymers. First, the potential effects of molecular motions were investigated by monitoring the conventional ^{13}C CPMAS NMR spectra of these samples as a function of temperature. Two main types of changes were revealed by these spectra (Figure 6): an onset of phenyl ring rotations which clearly influenced the 2,2′ carbon splitting in both polymers, and a conformational averaging of the aliphatic and methoxy resonances of the $n = 5$ sample which collapsed them into a distinct set of α, β, γ singlets at higher temper-

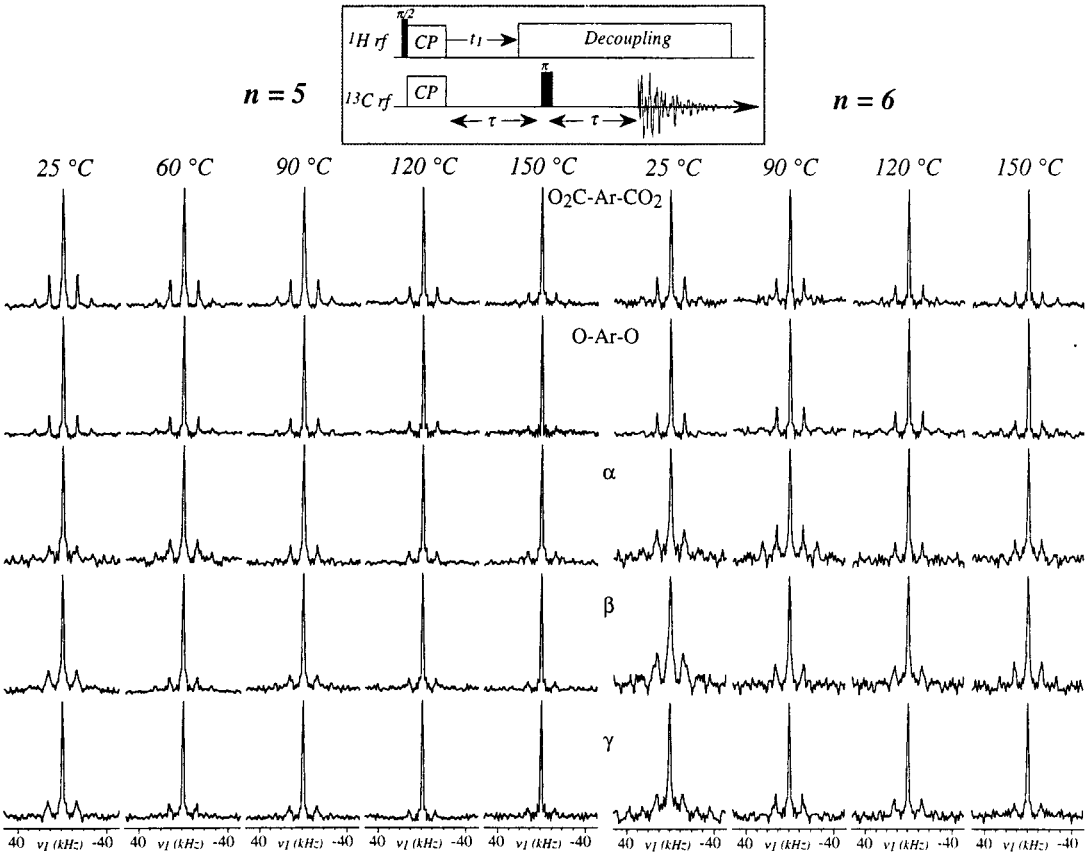

Figure 7. Variable-temperature separate-local-field line shapes observed for the indicated sites of the $n = 5$, 6 LCPs. The motion-induced decrease of the individual sidebands is indicative of the onset of large-amplitude reorientations occurring at rates that are typically greater than ≈40 kHz for methine and methylenes. The nature of these moderately fast-spinning (12 kHz) 2D SLF experiments has been described elsewhere;[31] during the present study a complete decay of the dipolar evolution was allowed to proceed in order to better characterize the distribution of motional dynamics (pulse sequence on inset; top). Hence 44 data sets with t_1 increments of 9.7 μs were taken while keeping the echo time τ constant at five rotor periods. 512 scans per t_1 point, a recycle delay of 3 s, and other acquisition conditions as described in Figure 6 were used in these variable-temperature experiments.

atures. Contrasting this behavior, no significant dynamics were observed for the $n = 6$ alkyl chains. In terms of temperature sensitivity, both aromatic and aliphatic averaging processes indicate a higher mobility for the $n = 5$ polymer as compared to its $n = 6$ counterpart.

A tighter, more rigid lattice packing was also revealed for the $n = 6$ sample by 2D separate-local-field variable-temperature NMR experiments, which monitor the dipolar couplings between directly bonded $^{13}C-^{1}H$ spin pairs at each of the polymers' positions. Figure 7 shows a series of such sideband line shapes extracted for selected sites in both $n = 5$ and $n = 6$ polymers, at temperatures ranging from 25 to 150 °C. At room temperature and for the aromatic terephthalate sites of both samples, the $^{13}C-^{1}H$ spinning sidebands have the typical intensity profiles that could be expected from static aromatic bonds. Yet for all other instances the sideband intensities are smaller than expected, indicating the onset of molecular motions at rates equal to or exceeding the heteronuclear coupling (≈40 kHz). Furthermore, for every inequivalent carbon site the local field data for the $n = 6$ polymer show at any given temperature a stronger $^{13}C-^{1}H$ coupling than for the $n = 5$ sample. This relatively higher degree of rigidity for the $n = 6$ polymer is seen particularly clear at the higher temperatures, e.g., at 150 °C, where its $^{13}C-^{1}H$ sidebands are still fairly intense for most sites whereas those of the $n = 5$ polymer have essentially been averaged to zero by fast molecular motions. Again, these dynamic differences between even- and odd-numbered LCPs are consistent with a tighter packing for the former. The spectra also indicate that for both $n = 5$ and $n = 6$ samples the methylene spacers have a higher degree of mobility than the mesogenic core and that this mobility increases for the central γ sites. Line shapes even suggest dynamics that for both LCPs are more extensive in the outer O−Ar−O rings than in the interior $O_2C-Ar-CO_2$ group. Finally, it is worth noting that, as also the case with the CPMAS spectra, the variations shown by all these 2D data are continuous and do not reveal any evident exchange broadening; such behavior is typical of heterogeneous systems involving a range of dynamic rates at any given temperature.

4. Conclusions

^{13}C NMR techniques were employed in a variety of complementary ways in order to retrieve information about how conformation, order, and dynamics change within a thermotropic LCP series as a function of monomeric structure. From an experimental standpoint common denominators among the various methods assayed were their simplicity, good S/N, and reliance on a natural abundance spectroscopic probe. These features enabled us to investigate a variety of samples under different conditions, thereby opening a window to explore how the alkyl spacer's length controls micro- and macroscopic properties in LCP polyesters. At a microscopic level, the CPMAS and variable-temperature experiments revealed a conformationaly more homogeneous and a less dynamic nature for the even-chained than for the odd-chained polymer structures. This trend was also detected at a bulk level by the variable-director experiments, which showed orientational distributions σ_θ that were nearly twice as wide for $n =$ odd polymers than for $n =$ even. These semiquantitative findings could be rationalized in terms of traditional even−odd packing effects, which arise as important factors in defining the properties of these semiflexible main-chain thermotropic polymers. Other interesting molecular details revealed by the local field ^{13}C NMR data include the onset of extensive reorientations in the aliphatic spacers of all LCPs as temperature was raised toward the nematic transition point and evidence that these motions become less restricted as sites depart within the monomer from the mesogenic core. Unfortunately, the line shape changes afforded by these methods are still too ambiguous to pinpoint the actual nature of the motions or their rate distributions. To elucidate these details, a series of spin-labeled LCPs have been synthesized from which new insight is expected to emerge via recoupling-based dipolar measurements.

Acknowledgment. We are grateful to Dr. Min Zhou for his assistance in recording the polymers' VACSY data. This work was supported by the U.S. National Science Foundation through Grant DMR-9806810, by the U.S. Department of Energy through Grant 00ER-15049, and by a Philip M. Klutznick Fund for Research (Weizmann Institute).

References and Notes

(1) Samulski, E. T. *Phys. Today* **1982**, *35*, 40.
(2) *Polymer Liquid Crystals*; Ciferri, A., Krigbaum, W. R., Meyer, R. B., Eds.; Academic Press: New York, 1982.
(3) Finkelmann, H. *Angew. Chem., Int. Ed. Engl.* **1987**, *26*, 816.
(4) Kwolek, S. L.; Morgan, P. W.; Schaefgen, J. R. In *Encyclopedia of Polymer Science and Engineering*; Wiley: New York, 1988; Vol. 9, Chapter 1.
(5) Yang, H. H. *Aromatic High-Strength Fibers*; Wiley: New York, 1989.
(6) *Liquid Crystalline Polymers*; Carfagna, C., Ed.; Pergamon Press: Oxford, 1994.
(7) *Liquid Crystalline Polymers: Technological Advances*; Isagev, A. I., Kyu, T., Cheng, S. Z. D., Eds.; American Chemical Society: Washington, DC, 1996.
(8) Finkleman, H.; Rehage, C. *Makromol. Chem., Rapid Commun.* **1980**, *1*, 733.
(9) Ringsdorf, H.; Schneller, A. *Makromol. Chem., Rapid Commun.* **1982**, *3*, 557.
(10) *Liquid Crystal Polymers*; Gordon, M., Cantou, H.-J., Eds.; 1984; Vols. 59−61.
(11) Blackwell, J.; Biswas, A. In *Developments in Oriented Polymers*; Ward, I. M., Ed.; Elsevier: London, 1987; Vol. 2; p 153 and ff.
(12) Antoun, S.; Lenz, R. W.; Jin, J.-I. *J. Polym. Sci., Polym. Chem. Ed.* **1981**, *19*, 1901.
(13) Jo, B.-W.; Jin, J.-I.; Lenz, R. W. *Eur. Polym. J.* **1982**, *18*, 233.
(14) Maret, G.; Blumstein, A. *Mol. Cryst. Liq. Cryst.* **1982**, *88*, 295.
(15) Lenz, R. W.; Adduci, J.; Facinelli, J. V.; Pardey, R.; Shen, D.; Gabori, A.; Harris, F. W.; Cheng, S. T. D. *Macromolecules* **1993**, *26*, 3687.
(16) Campoy, I. *Spectrochim. Acta* **1996**, *52A*, 619.
(17) Campoy, I. *Vib. Spectrosc.* **1996**, *13*, 99.
(18) Uryu, T.; Kato, T. *Macromolecules* **1988**, *21*, 378.
(19) Kato, T.; Kabir, G.; Uryu, T. *J. Polym. Sci., Polym. Chem. Ed.* **1989**, *27*, 1447.
(20) Griffin, A. C.; Havens, S. J. *J. Polym. Sci., Polym. Phys. Ed.* **1981**, *19*, 951.
(21) Henrichs, P. M. *Macromolecules* **1987**, *20*, 2099.
(22) Hughes, C. D.; Sherwood, M. H.; Alderman, D. W.; Grant, D. M. *J. Magn. Reson. A* **1993**, *102*, 58.
(23) Chmelka, B. F.; Schmidt-Rohr, K.; Spiess, H. W. *Macromolecules* **1993**, *26*, 378.
(24) Harbison, G. S.; Vogt, V.-D.; Spiess, H. W. *J. Chem. Phys.* **1987**, *86*, 1206.
(25) Sachleben, J. R.; Frydman, L. *Solid State NMR* **1997**, *7*, 301.
(26) Frydman, L.; Chingas, G. C.; Lee, Y. K.; Grandinetti, P. J.; Eastman, M. A.; Barrall, G. A.; Pines, A. *J. Chem. Phys.* **1992**, *97*, 4800.

(27) Munowitz, M. G.; Griffin, R. G.; Bodenhausen, G.; Wang, T. H. *J. Am. Chem. Soc.* **1981**, *103*, 2529.
(28) Munowitz, M. G.; Griffin, R. G. *J. Chem. Phys.* **1982**, *76*, 2848.
(29) Schaefer, J.; McKay, R. A.; Stejskal, E. O.; Dixon, W. T. *J. Magn. Reson.* **1983**, *52*, 123.
(30) Schaefer, J.; Stejskal, E. O.; McKay, R. A.; Dixon, W. T. *Macromolecules* **1984**, *17*, 1479.
(31) McElheny, D.; deVita, E.; Frydman, L. *J. Magn. Reson.* **2000**, *143*, 321.
(32) Facelli, J. C.; Grant, D. M. In *Topics in Stereochemistry*; Eliel, E., Wilen, S. H., Eds.; Wiley: New York, 1989; Chapter 1.
(33) Schmidt-Rohr, K.; Spiess, H. W. *Multidimensional Solid-State NMR and Polymers*; Academic Press: London, 1994.
(34) Ward, I. M. *Developments in Oriented Polymers*; Elsevier: London, 1982.
(35) Samulski, E. T.; Gauthier, M. M.; Blumstein, R. B.; Blumstein, A. *Macromolecules* **1984**, *17*, 479.
(36) Martins, A. F.; Ferreira, F. V.; Blumstein, A.; Blumstein, R. B. *Macromolecules* **1984**, *17*, 479.
(37) Abe, A. *Macromolecules* **1984**, *17*, 2280.

MA011863V